

# Robust Functional Principal Component Analysis for Non-Gaussian Continuous Data to Analyze Physical Activity Data Generated by Accelerometers

Rou Zhong<sup>a</sup>, Shishi Liu<sup>a</sup>, Haocheng Li<sup>b</sup>, and Jingxiao Zhang <sup>\*a</sup>

<sup>a</sup>Center for Applied Statistics, School of Statistics, Renmin University of China

<sup>b</sup>Department of Mathematics and Statistics, University of Calgary

## Abstract

Motivated by energy expenditure observations measured by wearable device, we propose two functional principal component analysis (FPCA) methods, Spearman FPCA and Kendall FPCA, for non-Gaussian continuous data. The energy expenditure records measured during physical activity can be modeled as functional data. They often involve non-Gaussian features, where the classical FPCA could be invalid. To handle this issue, we develop two robust FPCA estimators using the framework of rank statistics. Via an extension of the Spearman's rank correlation estimator and the Kendall's  $\tau$  correlation estimator, a robust algorithm for FPCA is developed to fit the model. The two estimators are applied to analyze the physical activity data collected by a wearable accelerometer monitor. The effectiveness of the proposed methods is also demonstrated through a comprehensive simulation study.

**Keywords:** Functional data analysis, functional principal component analysis, non-Gaussian process, Spearman's rank correlation, Kendall's  $\tau$  correlation

## 1 Introduction

Functional principal component analysis (FPCA), as a crucial technique in functional data analysis (FDA), is widely used in reducing dimensionality and exploring the major variation modes of sample curves. A comprehensive introduction on FPCA is provided in the monograph

---

<sup>\*</sup>zhjxiaoruc@163.com

by Ramsay and Silverman [Ramsay and Silverman \[2005\]](#). There is an extensive literature on the work of FPCA. To list a few, Yao and Lee [Yao and Lee \[2006\]](#) studied penalized spline models for FPCA. Chen and Lei [Chen and Lei \[2015\]](#) proposed a localized FPCA method to gain eigenfunctions with localized support regions. A dynamic FPCA approach was developed by Hörmann et al. [Hörmann et al. \[2015\]](#) with regard to functional time series. Moreover, Chiou et al. [Chiou et al. \[2014\]](#) and Wong et al. [Wong et al. \[2019\]](#) considered FPCA for multivariate functional data. However, these FPCA approaches may depend on the Gaussian process assumption either explicitly or implicitly. Further, Kraus and Panaretos [Kraus and Panaretos \[2012\]](#) have pointed out that the regular FPCA method would lead to biased outcomes for non-Gaussian continuous data, which coincides with our simulation study.

Meanwhile, non-Gaussian continuous data frequently occur in practice. For example, the physical activity data [Kozey-Keadle et al. \[2014\]](#), which motivated our study, are shown to be non-Gaussian (see Section 4). The data were obtained from 63 moderately overweight but healthy office workers in a health research project to increase exercise activities and reduce sedentary behaviors. Energy expenditure measurements were collected during physical activity for individuals over time. The primary outcome was energy expenditure level in the unit of metabolic equivalents (METs), which was a continuous variable. More specifically, this outcome was measured by every five minutes consecutively for three hours in each study participant, and thus each subject had 36 observations. Those measurements bear some skewed characteristics and contain a few extreme values, which imply a plain deviation from Gaussian distribution. In addition, besides the physical activity data, the DNA minicircles data [\[Kraus and Panaretos, 2012\]](#) and the Alzheimer's disease neuroimaging initiative (ADNI) data [\[Zhong et al., 2020\]](#) also show some non-Gaussian features. The goal of this article is to develop robust FPCA estimators for such non-Gaussian cases.

Recently, the study of FPCA for non-Gaussian data has attracted increasing attention. Hall et al. [Hall et al. \[2008\]](#) introduced a latent Gaussian process model for non-Gaussian longitudinal data that measured sparsely and irregularly. Van der Linde [van der Linde. \[2009\]](#) discussed a Bayesian FPCA approach for data in single-parameter exponential family. Gertheiss et al. [Gertheiss et al. \[2017\]](#) considered a generalized additive mixed model (GAMM) framework, and Li et al. [Li et al. \[2018\]](#) proposed an exponential family FPCA method. However, all of these studies were developed based on the assumption that data are generated from a specified distribution. These method may particularly work for discrete data (e.g. binary and count data), whereas it is difficult to assume a proper distribution for the physical activity records on hand.

In this paper, we propose a generalized FPCA method to handle continuous data without any distributional assumptions. The main idea is using rank statistics to replace the sample

covariance function, which is commonly implemented in the eigenanalysis for regular multivariate PCA [Han and Liu, 2014, 2018]. We use Spearman’s rank correlation estimator and Kendall’s  $\tau$  correlation estimator to construct new association functions. Moreover, a new algorithm is developed to conduct the Spearman FPCA and the Kendall FPCA with the newly established association functions. Our method does not involve any assumption of data distribution, which avoids model misspecification in real practice. In addition, the computation for the Spearman FPCA and the Kendall FPCA is convenient because it does not require taking multiple iterations to estimate non-Gaussian continuous functional data [Li et al., 2014].

The remainder of the article is organized as follows. Section 2 describes the two rank statistics and the newly developed algorithm for FPCA. Section 3 reports the results from simulation studies. Section 4 illustrates the application of our proposed methods to the physical activity data. Concluding discussions are provided in Section 5.

## 2 Method

Let  $X(t)$  denote a smooth random function evaluated at time  $t$  ( $t \in \mathcal{T}$ ), with unknown mean function  $E\{X(t)\} = \mu(t)$  and covariance function  $\Gamma(t_1, t_2) = \text{cov}\{X(t_1), X(t_2)\}$  ( $t_1 \in \mathcal{T}, t_2 \in \mathcal{T}$ ). Define  $\Gamma$  as a covariance operator that  $(\Gamma\phi)(t_1) = \int \Gamma(t_1, t_2)\phi(t_2)dt_2$  with  $\phi(t)$  being an arbitrary function. A commonly used approach to implement FPCA is the eigenanalysis for  $\Gamma(t_1, t_2)$  [Ramsay and Silverman, 2005]. This method uses a set of orthogonal eigenfunctions  $\{\phi_1(t), \phi_2(t), \dots\}$  with the eigenequations

$$(\Gamma\phi_k)(t) = \lambda_k\phi_k(t), \quad k = 1, 2, \dots,$$

where  $\lambda_k$  is the  $k$ -th eigenvalue and  $\lambda_1 \geq \lambda_2 \geq \dots$ . In classical FPCA,  $X(t)$  can be expressed by the Karhunen-Loève expansion,

$$X(t) = \mu(t) + \sum_{k=1}^{\infty} \xi_k \phi_k(t), \quad (1)$$

where  $\xi_k$  is the  $k$ -th functional principal component score.  $\xi_1, \xi_2, \dots$  are uncorrelated random variables with mean 0 and variance  $\lambda_1, \lambda_2, \dots$ , respectively. The model fit for  $X(t)$  is equivalent to estimate  $\hat{\mu}(t)$ ,  $\hat{\lambda}_k$  and  $\hat{\phi}_k(t)$ . To be specific,  $\hat{\phi}_k(t)$  can be obtained from the estimate of the covariance function  $\Gamma(t_1, t_2)$ . Therefore, the estimation of  $\Gamma(t_1, t_2)$  plays an important role in FPCA.

Suppose we observe a set of independent random curves  $X_i(t)$  ( $i = 1, 2, \dots, N$ ) from  $N$  individuals. To accommodate the application data illustrated in Section 1, we assume all of the sample curves are recorded at a grid of  $d$  time points ( $t = 1, \dots, d$ ) in this paper. In

particular, we have  $d = 36$  in the physical activity data. Therefore, our methodology developed for the application problem assumes functional data with a equally-spaced and dense design. In Section 5, we discuss the approaches to extend our methods for more general settings.

The classical FPCA method estimates  $\Gamma(t_1, t_2)$  ( $1 \leq t_1 \leq d, 1 \leq t_2 \leq d$ ) by sample covariance function

$$\widehat{\Gamma}(t_1, t_2) = \frac{1}{N} \sum_{i=1}^N \{X_i(t_1) - \widehat{\mu}(t_1)\} \{X_i(t_2) - \widehat{\mu}(t_2)\}, \quad (2)$$

where  $\widehat{\mu}(t)$  is the sample mean function. It can be estimated by  $\widehat{\mu}(t) = \frac{1}{N} \sum_{i=1}^N X_i(t)$ . When continuous data follow Gaussian process, the classical FPCA method based on  $\widehat{\Gamma}(t_1, t_2)$  in (2) has good properties such as consistency and asymptotic efficiency property [Yao et al., 2005, Hall et al., 2006]. On the contrary, the results are implausible when facing non-Gaussian cases Kraus and Panaretos [2012]. Further, we also demonstrate in Section 3, the  $\widehat{\Gamma}(t_1, t_2)$  calculated in (2) with non-Gaussian features ignored, could lead to severely biased results. However, non-Gaussian features may occur frequently in real practice. For example, a dataset could be skewed and has outliers. To solve this problem, we consider two robust statistics to replace  $\widehat{\Gamma}(t_1, t_2)$  in Section 2.1 and Section 2.2, respectively.

## 2.1 Spearman FPCA

The implementation of the Spearman's rank correlation to the FPCA problem is based on its well-known robustness property to handle outliers in observations. It has good performance in heavy-tailed distributions [de Winter and Gosling, 2016], and thus it is appropriate to be applied in our physical activity data discussed in Section 1. In this section, we generalize the Spearman's rank correlation to handle functional data analysis.

For subject  $i$ , let  $r_i(t)$  represent the rank of  $X_i(t)$  among  $\{X_1(t), \dots, X_i(t), \dots, X_N(t)\}$ . Define  $\bar{r}(t) = \sum_{i=1}^N r_i(t)/N$ . The sample Spearman's rank correlation function is estimated as

$$\widehat{\rho}(t_1, t_2) = \frac{\sum_{i=1}^N \{r_i(t_1) - \bar{r}(t_1)\} \{r_i(t_2) - \bar{r}(t_2)\}}{\sqrt{\sum_{i=1}^N \{r_i(t_1) - \bar{r}(t_1)\}^2 \cdot \sum_{i=1}^N \{r_i(t_2) - \bar{r}(t_2)\}^2}}.$$

We use the following estimator in our application

$$\widehat{S}(t_1, t_2) = 2 \sin \left\{ \frac{\pi}{6} \widehat{\rho}(t_1, t_2) \right\}, \quad (3)$$

and the new eigenproblem is given by

$$(\widehat{S}\phi_k^S)(t) = \lambda_k^S \phi_k^S(t), \quad (4)$$

where  $\lambda_k^S$  and  $\phi_k^S(t)$  are the  $k$ -th eigenvalue and eigenfunction for the Spearman's rank correlation function, respectively.

## 2.2 Kendall FPCA

Follow the similar idea of the Spearman FPCA in Section 2.1, we introduce the Kendall's  $\tau$  into the functional data analysis. A straightforward Kendall correlation function can be estimated as

$$\widehat{K}_0(t_1, t_2) = \frac{2}{N(N-1)} \sum_{i < j} [\text{sign}\{X_i(t_1) - X_j(t_1)\} \text{sign}\{X_i(t_2) - X_j(t_2)\}],$$

where  $\text{sign}(\cdot)$  is the sign function. However, the estimated  $\widehat{K}_0(t_1, t_2)$  could be numerically unstable in our simulation studies and data applications. The numerical instability problem leads to difficulties in model computation and explanation. Therefore, we use the approach discussed in Croux et al. [Croux et al. \[2002\]](#) to define a new correlation function

$$\widehat{K}(t_1, t_2) = \frac{2}{N(N-1)} \sum_{i < j} \frac{\{X_i(t_1) - X_j(t_1)\} \{X_i(t_2) - X_j(t_2)\}}{\|X_i - X_j\|^2}, \quad (5)$$

where  $\|X_i - X_j\|^2 = \int_{\mathcal{T}} \{X_i(u) - X_j(u)\}^2 du$ .

The eigenproblem for Kendall FPCA is

$$(\widehat{K}\phi_k^K)(t) = \lambda_k^K \phi_k^K(t), \quad (6)$$

where  $\lambda_k^K$  and  $\phi_k^K(t)$  are the  $k$ -th eigenvalue and eigenfunction for the Kendall correlation function, respectively.

## 2.3 Computation

In this section, we illustrate the algorithm to implement the Spearman FPCA discussed in Section 2.1. The algorithm can be summarized as follows:

**Step 1.** Estimate  $\mu(t)$  by

$$\widehat{\mu}(t) = \frac{1}{N} \sum_{i=1}^N X_i(t).$$

**Step 2.** Calculate the sample correlation function  $\widehat{S}(t_1, t_2)$  by (3) for  $t_1 = 1, \dots, d$  and  $t_2 = 1, \dots, d$ .

**Step 3.** Based on the method with penalization for roughness proposed by Rice and Silverman [Rice and Silverman \[1991\]](#), calculate the estimated vector  $\widetilde{u}_1^S = \{\widehat{\phi}_1^S(1), \dots, \widehat{\phi}_1^S(d)\}$ .

**Step 4.** Follow the similar pattern, sequentially calculate  $\widetilde{u}_2^S$ ,  $\widetilde{u}_3^S$ , and the vectors for higher order eigenfunctions.

**Step 5.** Recover the estimated functions  $\tilde{\phi}_k^S(t)$  from  $\tilde{u}_k^S$  by using B-spline basis functions.

**Step 6.** We obtain the  $\hat{\phi}_k^S(t)$  by

$$\hat{\phi}_k^S(t) = \frac{\tilde{\phi}_k^S(t)}{\|\tilde{\phi}_k^S\|},$$

$$\text{where } \|\tilde{\phi}_k^S\| = \sqrt{\int_{\mathcal{T}} \{\tilde{\phi}_k^S(u)\}^2 du}.$$

The Kendall FPCA discussed in Section 2.2 can be implemented from the similar approach by substituting  $\hat{S}(t_1, t_2)$  with  $\hat{K}(t_1, t_2)$  in (5) to obtain the estimation of  $\hat{\phi}_k^K(t)$ .

### 3 Simulation Studies

In this section, we use a simulation study to demonstrate the performance of our proposed Spearman FPCA and Kendall FPCA. As a comparison, the classical FPCA approach is also explored. In the simulation study of 100 runs, we have  $N = 100$  individuals and each subject has  $d = 100$  equally-spaced observations. Here we generate the data using the discretized covariance function rather than using the expansion (1). For Scenario 1, the covariance function is set to be

$$\Gamma(t_1, t_2) = 15\phi_1(t_1)\phi_1(t_2) + 5\phi_2(t_1)\phi_2(t_2) + I(t_1 = t_2), \quad t_1, t_2 \in [0, 10], \quad (7)$$

where  $I(t_1, t_2) = 1$  if  $t_1 = t_2$ ; otherwise  $I(t_1, t_2) = 0$ . The two leading eigenfunctions are  $\phi_1(t) = \sin(\pi t/5)/\sqrt{5}$  and  $\phi_2(t) = \cos(\pi t/5)/\sqrt{5}$ , respectively. For Scenario 2, the covariance function is set to be

$$\Gamma(t_1, t_2) = \min\{t_1, t_2\} - t_1 t_2, \quad t_1, t_2 \in [0, 1], \quad (8)$$

where the two leading eigenfunctions can be derived as  $\phi_1(t) = \sqrt{2}\sin(\pi t)$  and  $\phi_2(t) = \sqrt{2}\sin(2\pi t)$ .

For both scenarios, data are generated from Gaussian distribution, student's  $t$  distribution, and skew- $t$  distribution [Azzalini and Genton, 2008] using the covariance functions specified in (7) and (8), respectively. For Gaussian distribution, we set the mean to be zero. For student's  $t$  distribution, the degree of freedom is set to be three. For skew- $t$  distribution, location parameter is set to be zero, slant parameter is defined to be 10, and the degree of freedom is three. For the estimates of each simulation run, the following criteria are evaluated to assess the performance of the three methods:

- $Err_k = \int \{\phi_k(t) - \hat{\phi}_k(t)\}^2 dt$ . The  $Err_k$  measures the estimation error for the  $k$ -th eigenfunction.

- $\text{Angle}_k = \arccos(|\int [\phi_k(t)\hat{\phi}_k(t)]dt|)$ . The  $\text{Angle}_k$ , which ranges from 0 to 90, presents the angle size of the  $k$ -th estimated eigenfunction deviated from the true one. Specifically, smaller  $\text{Angle}_k$  means better estimation.

Figure 1 displays the simulation results of  $\hat{\phi}_k(t)$  using the classical FPCA, the Spearman FPCA and the Kendall FPCA methods for Scenario 1. Three approaches have similar estimates, which are close to true curves under Gaussian distribution and student's  $t$  distribution. However, the classical FPCA approach leads to obvious biased estimates under skew- $t$  distribution settings. Figure 2 illustrates the simulation results for Scenario 2. It can be seen that the classical FPCA performs well under Gaussian distribution. Our proposed Spearman FPCA and Kendall FPCA methods have very small bias but the estimates are still comparable to the classical FPCA's outcomes. On the other hand, the classical FPCA approach yields remarkably biased estimates for the student's  $t$  and skew- $t$  distributions, while our Spearman FPCA and Kendall FPCA approaches lead to satisfactory curve estimates.

Table 1 shows the  $Err_k$  and  $\text{Angle}_k$  ( $k = 1, 2$ ) for Scenarios 1 and 2, respectively. For the Gaussian distribution settings, our Spearman FPCA and Kendall FPCA approaches generally lead to similar outcomes as the classical FPCA. In the settings of student's  $t$  and skew- $t$  distributions, the two proposed methods lead to obvious smaller deviance to the true curves compared to the classical FPCA method. Therefore, the simulation results suggest that the classical FPCA, may provide misleading conclusions under non-Gaussian data settings. On the other hand, our proposed robust methods have satisfactory estimation results for different scenarios.

## 4 Application

In this section we use the proposed method to analyze the physical activity dataset collected by wearable monitors [Kozey-Keadle et al. \[2014\]](#). The raw activity signal is captured by a device named the ActivPAL<sup>TM</sup> ([www.paltech.plus.com](http://www.paltech.plus.com)). This device is taped in front of the thigh. It uses an accelerometer to measure the angle of the thigh and the movement speed. The raw data recorded by the accelerometer are used to calculate energy expenditure level in metabolic equivalents (METs). In general, physical activity with METs  $< 3$  can be identified as light activity; otherwise, it is moderate-to-vigorous activity. The dataset has  $N = 63$  subjects and each participant has  $d = 36$  five-minute interval records. Figure 3(a) shows the energy expenditure observation from one subject across three hours. Figure 3(b) shows the histogram of the observations from all subjects. Figures 3(c)-(f) are histograms and Q-Q plots for the energy expenditure level at two time points. The plots suggest the continuous variable is skewed and has extreme values.

In this application,  $X_i(t)$  can be defined as the continuous variable for energy expenditure level in the  $t^{th}$  ( $t = 1, \dots, 36$ ) five-minute interval from subject  $i$  ( $i = 1, \dots, 63$ ). Our proposed Spearman FPCA and Kendall FPCA approaches are used to analyze the physical activity dataset as the non-Gaussian features, which includes right skewness and extreme values, must be taken into account. Figure 4(a) illustrates that mean energy expenditure level slightly increases at  $t = 1$  and then decreases back to starting level at about  $t = 5$ . The light energy expenditure could be explained as the warming up stage designed in this health research project to reduce the risk of injury. The METs level increases dramatically at about  $t = 12$ , and decreases back to just above the starting level by  $t = 24$ . During this interval, individuals take an intense exercise training for about 30 minutes and then start to cool down for about 25 minutes. The energy expenditure level stays the same after  $t = 24$ , which shows subjects are taking sedentary activities after the exercise program. Figures 4(b)(c) display the estimates of the first two eigenfunctions. For Kendall FPCA, the first eigenfunction rises to a peak at about  $t = 16$ , and then decreases to zero. This suggests that main pattern of the variability in energy expenditure is around  $t = 16$  across different participants. Subjects would have highly different METs level during the intense exercise program because they have various physical training experience. On the other hand, the second eigenfunction has one positive and one negative peaks, which indicates energy expenditure variabilities at  $t = 15$  and  $t = 21$  are negatively correlated. That is, if a subject spends higher energy expenditure around  $t = 15$ , he/she may have lower energy expenditure later. The estimated eigenfunctions from the Spearman FPCA have similar patterns as the Kendall FPCA's estimates, while the first eigenfunction has slower decreasing trend and the second eigenfunction suggests larger variance between  $t = 1$  to  $t = 5$ .

## 5 Conclusion and Discussion

In this paper, we developed the Spearman FPCA and the Kendall FPCA methods to analyze functional data in non-Gaussian cases. The two robust methods are developed using two rank statistics, Spearman's rank correlation and Kendall's  $\tau$  correlation, respectively. The simulation results are encouraging. Our methods have comparable results to the classical FPCA method under Gaussian settings. For non-Gaussian cases, our proposed approaches have little bias and outperform the classical FPCA. The analysis of the physical activity data based on the developed method demonstrates their utility in real world data applications.

In this paper, the functional data are assumed to have regular and dense structure. It is of interest to generalize the two methods to irregular and sparse cases. For example, we may extend our methods to sparse cases by using the local linear estimation [Yao et al., 2005]. Moreover, we can explore other correlation measurements to handle FPCA problems in future

studies.

## Acknowledgement

Li was supported by discovery grants program from the Natural Sciences and Engineering Research Council of Canada (NSERC, RGPIN-2015-04409). The authors thank Dr. Sarah Kozey Keadle for making the physical activity data available to them. Dr. Sarah Kozey Keadle was supported by a National Cancer Institute grant (R01-CA121005).

## References

J. O. Ramsay and B. W. Silverman. *Functional Data Analysis (2nd ed.)*. Springer Series in Statistics, New York: Springer, 2005.

Fang Yao and Thomas C. M. Lee. Penalized spline models for functional principal component analysis. *Journal of the Royal Statistical Society. Series B (Methodological)*, 68:3–25, 2006.

Kehui Chen and Jing Lei. Localized functional principal component analysis. *Journal of the American Statistical Association*, 110:511:1266–1275, 2015.

Siegfried Hörmann, Lukasz Kidziński, and Marc Hallin. Dynamic functional principal components. *Journal of the Royal Statistical Society. Series B (Methodological)*, 77:319–348, 2015.

Jeng-Min Chiou, Ya-Fang Yang, and Yu-Ting Chen. Multivariate functional principal component analysis: A normalization approach. *Statistica Sinica*, 24:1571–1596, 2014.

Raymond K. W. Wong, Yehua Li, and Zhengyuan Zhu. Partially linear functional additive models for multivariate functional data. *Journal of the American Statistical Association*, 114:525:406–418, 2019.

David Kraus and Victor M. Panaretos. Dispersion operators and resistant second-order functional data analysis. *Biometrika*, 99(4):813–832, 2012.

Sarah Kozey-Keadle, John Staudenmayer, Amanda Libertine, Marianna Mavilia, Kate Lyden, Barry Braun, and Patty Freedson. Changes in sedentary time and spontaneous physical activity in response to an exercise training and/or lifestyle intervention. *Journal of Physical Activity and Health*, 11:1324–1333, 2014.

Qingzhi Zhong, Huazhen Lin, and Yi Li. Cluster non-gaussian functional data. *Biometrics*, 2020. doi: <https://doi.org/10.1111/biom.13349>.

Peter Hall, Hans-Georg Müller, and Fang Yao. Modelling sparse generalized longitudinal observations with latent gaussian processes. *Journal of the Royal Statistical Society: Series B (Statistical Methodology)*, 70:703–723, 2008.

Angelika van der Linde. A bayesian latent variable approach to functional principal components analysis with binary and count data. *AStA Advances in Statistical Analysis*, 93:307–333, 2009.

Jan Gertheiss, Jeff Goldsmith, and Ana-Maria Staicu. A note on modeling sparse exponential-family functional response curves. *Computational Statistics and Data Analysis*, 105:46–52, 2017.

Gen Li, Huang, Jianhua Z. Huang, and Haipeng Shen. Exponential family functional data analysis via a low-rank model. *Biometrics*, 74:1301–1310, 2018.

Fang Han and Han Liu. High dimensional semiparametric scale-invariant principal component analysis. *IEEE Transactions on Pattern Analysis and Machine Intelligence*, 36:2016–2032, 2014.

Fang Han and Han Liu. Eca: High-dimensional elliptical component analysis in non-gaussian distributions. *Journal of the American Statistical Association*, 113:521:252–268, 2018.

Haocheng Li, John Staudenmayer, and Raymond J. Carroll. Hierarchical functional data with mixed continuous and binary measurements. *Biometrics*, 70:802–811, 2014.

Fang Yao, Hans-Georg Müller, and Jane-Ling Wang. Functional data analysis for sparse longitudinal data. *Journal of the American Statistical Association*, 100(470):577–590, 2005.

Peter Hall, Hans-Georg Müller, and Jane-Ling Wang. Properties of principal component methods for functional and longitudinal data analysis. *Annals of Statistics*, 34(3):1493–1517, 2006.

Joost C. F. de Winter and Samuel D. Gosling. Comparing the pearson and spearman correlation coefficients across distributions and sample sizes: A tutorial using simulations and empirical data. *Psychological Methods*, 21:273–290, 2016.

Christophe Croux, Esa Ollila, and Hannu Oja. Sign and rank covariance matrices statistical properties and application to principal components analysis. *Statistics for Industry and Technology*, pages 257–269, 2002.

John A. Rice and B. W. Silverman. Estimating the mean and covariance structure nonparametrically when the data are curves. *Journal of the Royal Statistical Society. Series B (Methodological)*, 53:233–243, 1991.

Adelchi Azzalini and Marc G. Genton. Robust likelihood methods based on the skew-t and related distributions. *International Statistical Review*, 76(1):106–129, 2008.

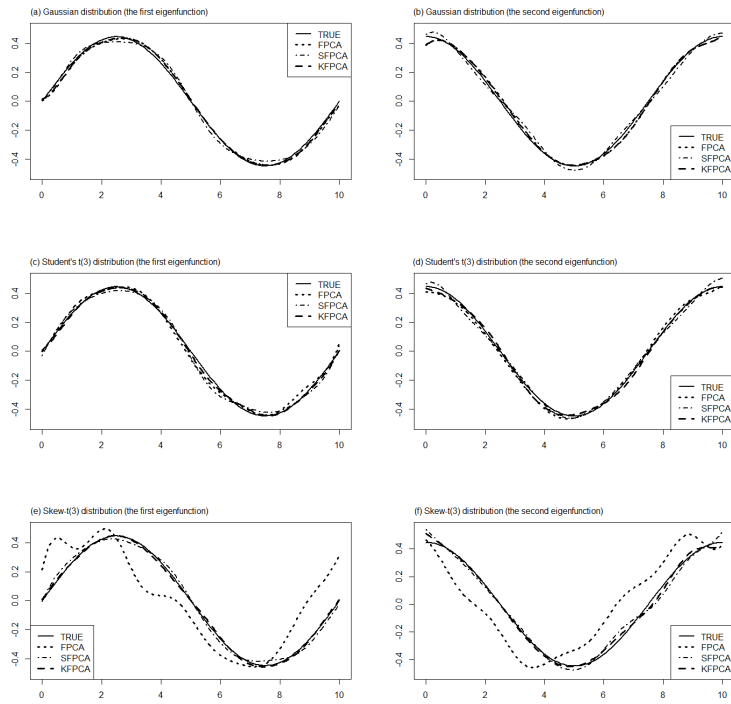


Figure 1: Eigenfunction estimations for 100 simulation runs in Scenario 1 illustrated in Section 3. (a)(b) The first and the second eigenfunctions for Gaussian distribution settings. (c)(d) The first and the second eigenfunctions for student's  $t$  distribution. (e)(f) The first and the second eigenfunctions for skew- $t$  distribution. Thick solid lines are for true curves. Dotted lines, dot-dashed lines, and dashed lines are for the classical FPCA, the Spearman FPCA and the Kendall FPCA methods, respectively.

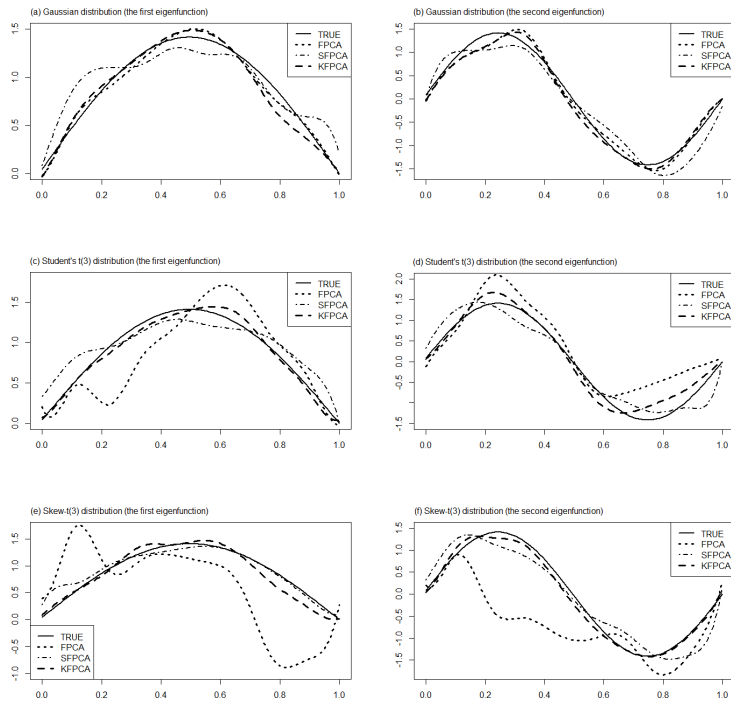


Figure 2: Eigenfunction estimations for 100 simulation runs in Scenario 2 illustrated in Section 3. (a)(b) The first and the second eigenfunctions for Gaussian distribution settings. (c)(d) The first and the second eigenfunctions for student's  $t$  distribution. (e)(f) The first and the second eigenfunctions for skew- $t$  distribution. Thick solid lines are for true curves. Dotted lines, dot-dashed lines, and dashed lines are for the classical FPCA, the Spearman FPCA and the Kendall FPCA methods, respectively.

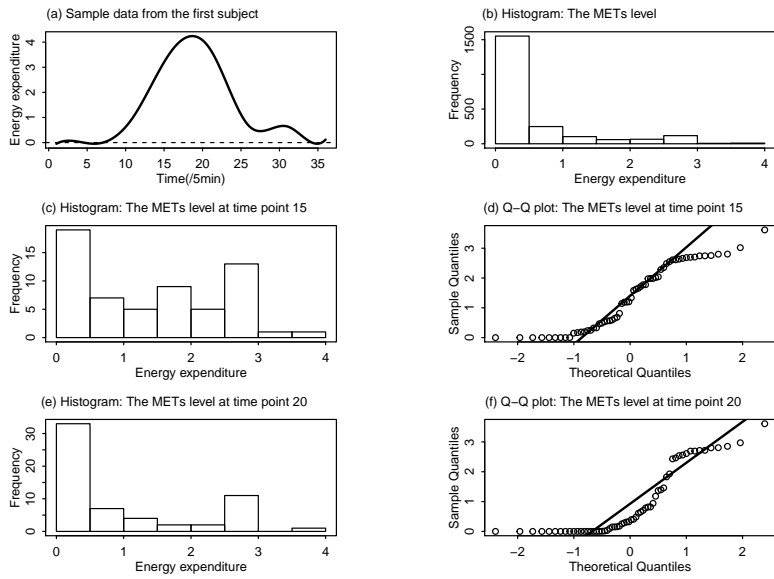


Figure 3: (a) Energy expenditure observation from subject with ID 1 across 3 hours. (b) Histogram of the energy expenditure observations (METs) from all subjects. (c)(d) Histogram and Q-Q plot for the energy expenditure level (METs) at time point 15. (e)(f) Histogram and Q-Q plot for the energy expenditure level (METs) at time point 20.

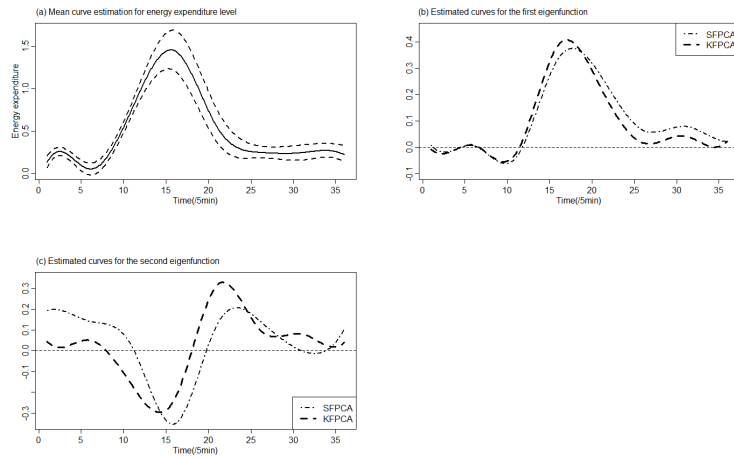


Figure 4: FPCA results for the physical activity data illustrated in Section 4. (a) Mean curve estimation for energy expenditure level. Solid line and dashed line are the estimated curve and its 90% bootstrap confidence intervals, respectively. (b)(c) Estimated curves for the first and the second eigenfunctions. Thin dot-dashed lines and thick dashed lines are the Spearman FPCA and the Kendall FPCA, respectively.

Table 1: Simulation results for the averaged  $Err_1$ ,  $Err_2$ ,  $Angle_1$  and  $Angle_2$  across 100 runs. The simulation settings and the definition of the  $Err_1$ ,  $Err_2$ ,  $Angle_1$  and  $Angle_2$  are illustrated in Section 3.

		Scenario 1			Scenario 2		
		FPCA	SFPCA	KFPCA	FPCA	SFPCA	KFPCA
Gaussian	$Err_1$	0.01	0.02	0.01	0.01	0.04	0.01
	$Err_2$	0.01	0.02	0.01	0.03	0.16	0.03
	$Angle_1$	4.36	7.59	4.53	4.78	11.85	5.03
	$Angle_2$	5.09	6.75	5.34	9.46	22.42	9.82
Student's $t(3)$	$Err_1$	0.06	0.02	0.01	0.06	0.04	0.01
	$Err_2$	0.06	0.02	0.01	0.20	0.15	0.04
	$Angle_1$	10.29	7.84	5.16	11.19	11.68	5.44
	$Angle_2$	11.40	7.59	5.93	22.52	22.19	11.36
Skew- $t(3)$	$Err_1$	0.07	0.02	0.01	0.17	0.09	0.08
	$Err_2$	0.07	0.02	0.01	0.24	0.15	0.08
	$Angle_1$	11.04	7.99	5.21	19.77	14.32	14.13
	$Angle_2$	12.19	7.62	6.19	24.60	20.62	14.36